Controlled Beam Migration – Application in Gulf of Mexico

Chu-Ong Ting, CGGVeritas
Daoliu Wang, CGGVeritas

This paper was prepared for presentation during the 11th International Congress of the Brazilian Geophysical Society held in Salvador, Brazil, August 24-28, 2009.

Abstract

In this paper we review the subsalt challenges and present a specialized beam migration to address the issues of steep dip imaging, multi-arrival capability, and S/N ratio enhancement. We show its applications in the Gulf of Mexico area, for both narrow azimuth and wide azimuth data.

Introduction

In the deep water Gulf of Mexico, the salt tectonics creates complicated salt bodies, including various shapes of salt sheet, salt canopy, and salt dome. This high velocity medium poses a serious challenge to seismic acquisition and imaging because its high velocity contrast to surrounding sediment field creates a lens that distorts the wave field propagation. As a result only a limited portion of the seismic energy is able to transmit down to the subsalt target, and even less is able to propagate back and to be received by seismic receivers at the surface, depending on the receiver coverage. In conventional narrow azimuth towed streamer (NAZ) acquisition, the receivers are layout in a 2D sense along the shooting direction so most reflected subsalt energy was not acquired in the data. The latest wide azimuth (WAZ) acquisition is designed to address this issue. Its receivers cover a much wider azimuth range, thus have a better chance to capture more reflected subsalt energy.

As for the challenges to imaging technology, it has been widely realized that three key components are required in order to deliver high quality subsalt images, i.e. a high accuracy prestack depth migration algorithm, an accurate velocity model (especially salt model) and good quality input data. Algorithms like prestack Kirchhoff depth migration have been the workhorse in the imaging industry until its single arrival approximation was recognized to be insufficient to deal with complex geology in the Gulf of Mexico subsalt play. As a result the primary reflections beneath the salt were often masked by migration artifacts, such as excessive migration swings found in the Kirchhoff images.

Due to these issues, one-way wave equation migration (WEM) is generally a preferred alternative algorithm over Kirchhoff migration in the subsalt imaging. It is able to account for all arrivals underneath the salt and able to handle structurally complex medium without loss of accuracy. However, it has problems in imaging steep or overturned events, and the extension to anisotropy media can be quite computationally inefficient. As a result of these pros and cons, it is quite common to utilize both algorithms throughout the model building phases of a subsalt imaging project so that interpreters will have both migrated volumes interpreted concurrently in order to build an accurate depth velocity model. This workflow sometimes can prolong the project cycle time which becomes problematic when the drilling schedule has been set. Moreover, none of these migration algorithms addresses the low signal-to-noise ratio issues in the recorded data, which is an important aspect issue when it comes to subsalt imaging.

Controlled Beam Migration

These issues led to the development of controlled beam migration (CBM) which is a specialized beam migration which not only is able to image steep dips or overturned events and has multi-arrivals capability, but is also able to enhance the signal-to-noise (S/N) ratio of the image.

CBM shares a similar theoretical basis as the most of the other beam migrations, which have been published by several authors (Alkhalifah, 1995; Hill, 2001; Albertin et al., 2001; Nowak et al., 2003; Gray, 2005; Zhu et al., 2005). Like general beam migrations, the data is subdivided into smaller patches and transformed into the tau-p domain in the beam forming process. The S/N ratio is enhanced in this domain as most of the incoherence events get suppressed by tau-p stacking, and thus gives a cleaner input for migration than in the case of Kirchhoff and WEM.

The data is then migrated using a multi-arrival, ray-based traveltime table and stacked together with other beams to form the output images. Since the migration algorithm is ray based, it suffers the same caustic issues as the Kirchhoff migration in complex regions. As a result, the accuracy of CBM falls in between the single-arrival Kirchhoff and one-way wave equation migration. On the other hand, since there is no dip limitation in the ray tracing, CBM is capable of imaging steeply dipping and overturned events, which is not offered by the one-way wave equation migration.

CBM had been tested and utilized in various areas at the Gulf of Mexico, and proved to be an effective tool to improve the S/N ratio of the image.

Applications of CBM in the Gulf of Mexico

We present two CBM applications in the Green Canyon and Walker Ridge area of the Gulf of Mexico.

In Figure 1, we compare images of three migration algorithms, Kirchhoff (left), WEM (middle) and CBM (right), in the southeast corner of Green Canyon. All the results are obtained using exactly the same input data and velocity model. The input data has been processed with the latest 3D SRME technology to reduce waterbottom and top of salt related surface multiples contamination. The complicated salt body with sutures and sediment inclusions poses a challenge to the single-arrival Kirchhoff migration, whose subsalt images is contaminated by migration swings. The WEM image in the middle is able to deliver stronger subsalt events with better continuity and less swing than that of Kirchhoff migration, but it still suffers from a low S/N ratio. In this case CBM is able to enhance the signal compared to the surrounding noise and gives more coherent subsalt events. Its multi-arrival capability also helps to produce an image with less swings than that of Kirchhoff.

In Figure 2, we further extend the Kirchhoff and CBM comparison to the common image gathers at the middle section of Figure 1. These common image gathers are the direct migration output without applying any post migration process. The interpreted base of salt is marked by the red arrow on the 2nd gather. As expected, the improvement of CBM over Kirchhoff is little above the base of salt where we have good data quality. In the subsalt region indicated by the black rectangle, stronger subsalt events with flat curvature can be easily identified in CBM gathers, while Kirchhoff gathers are masked by residue multiples. With cleaner stack and gathers, CBM offers a better input for automated residue curvature picking and thus will possibly yield more reliable velocity updates in both supra-salt and subsalt region than that of Kirchhoff.

We now extend our comparison from previous narrow azimuth data in Green Canyon to the recently acquired Jack development wide azimuth data (DWAZ) in Walker Ridge. The WAZ survey was acquired at a 45 degree NE-SW shooting direction by four source boats (two lead boat and two tail boats) and one streamer boat, with the multi-pass scheme, in order to achieve the maximum 4km crossline offset (or 4 “tiles”). The acquisition geometry is very close to what has been discussed in Michell et al., 2006, except the source line spacing is 500m in this case. The Jack DWAZ data can be naturally decomposed into vector offsets, with four crossline offsets at 1km increment (offset Y) and 54 inline offsets (offset X) at 300m increment. As a result, this yields a total of 216 high density offset volumes (216 fold).

Both WAZ WEM and WAZ CBM migrated images are shown at the top of Figure 3. For reference, at the bottom of Figure 3, we also add the CBM and WEM migration images from the legacy narrow azimuth data which were acquired in the EW shooting direction, and has a total offset fold of 40. All the images here are migrated with exactly the same legacy narrow azimuth data derived velocity model, in order to compare the effect of algorithms and input data. The NAZ comparison at the bottom shows both NAZ CBM and NAZ WEM fail to resolve the circled region caused by poor illumination. Even though NAZ CBM shows a clearer subsalt image than NAZ WEM, the circled events are still broken and curvy. Both WAZ WEM and WAZ CBM images shown at the top are able to resolve this region better than NAZ, and interestingly, given the high fold of the WAZ data, there is still benefit from CBM S/N enhancement in the circled area.

To investigate the poor NAZ image, we display one WAZ CBM migrated gather located at the center of the circled region in Figure 4. This 216 vectoroffset gather is displayed in two different ways, i.e. (a) 2D tiles panel and (b) 3D vector offset volume. In the 2D tiles panel view, the gather is grouped by tiles, from 1st tile to 4th tiles, and ordering from negative offset X to positive offset X within each tile. In the 3D vector offset volume, the gather is displayed in terms of inline offset (offset X) and crossline offset (offsetY), and one can follow the same event to different offsetY by sliding the cross-section. The 7.5km depth slice was taken at the event marked by the arrows in (a), and it is clear that this subsalt event appears only in a limited range of vector offset (equivalently, limited offset-azimuth range), which explains the illumination issue found in poor NAZ images. CBM ability of generating 3D vector offset gathers provides a useful QC for various illumination related issues and the input for the wide azimuth subsalt velocity update.

Conclusions

We have presented CBM as an alternative migration algorithm whose accuracy lies between Kirchhoff and one-way wave equation migration, and is able to deliver images with better S/N ratio as well as cleaner offset gathers for velocity update. In the case of WAZ data, it outputs vector offset gathers for 3D WAZ tomography inversion. However, it still faces the I/O and operational efficiency challenge brought by WAZ as well as the failure of ray tracing in more complicated salt region, which requires algorithms with higher fidelity like reverse time migration.

Acknowledgements

The authors would like to thank CGGVeritas for permission to publish this work. We also thank Jerry Young and Uzi Egozi for their thoughtful suggestions, Wei Zhao and Tim Schroeder for their CBM examples, and Bruce Ver West for reviewing the paper.

References

Albertin, U., Yingst, D., and Jaramillo, H., 2001, Comparing common-offset Maslov, Gaussian beam, and coherent state migration: 71st Annual International Meeting, SEG, Expanded Abstracts, 913-916.

Alkhalifah, T., 1995, Gaussian beam depth migration for anisotropic media: Geophysics, 20, 1474-1434.

Gray, S.H., 2005, Gaussian beam migration of common-shot records: Geophysics, 70, S71-S77.

Hill, N.R., 2001, Prestack Gaussian-beam depth migration: Geophysics, 22, 1240-1250.

Nowack, R.L., Sen, M.K., and Stoffa, P.L., 2003, Gaussian beam migration for sparse common-shot and common-receiver data: 73rd Annual International Meeting, SEG, Expanded Abstracts, 1114-117.

Zhu, T., Gray, S., and Wang, D., 2005, Kinematic and dynamic ray tracing in anisotropic media: theory and application: 75th Annual International Meeting, SEG, Expanded Abstracts, 96-99.

Michell, S., Shoshitaishvili, E., Chergotis, D., Sharp, J., Etgen, J.,2006, Wide azimuth streamer imaging of Mad Dog; Have we solved the Subsalt imaging problem?: 76th Internat. Mtg., Soc. Expl. Geophys., Expanded Abstracts, 2905-2909.

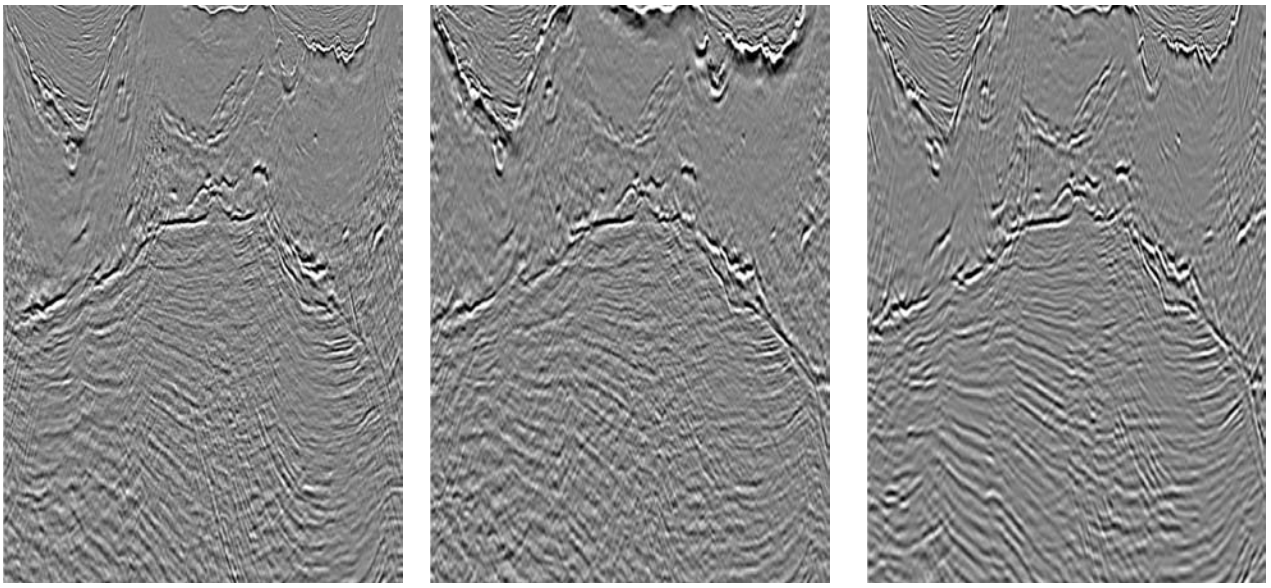

(a) Kirchhoff migration (b) Wave Equation Migration (c) Controlled Beam Migration

Figure 1: Comparison of images from (a) Kirchhoff , (b) Wave equation migration and (c) Controlled Beam Migration

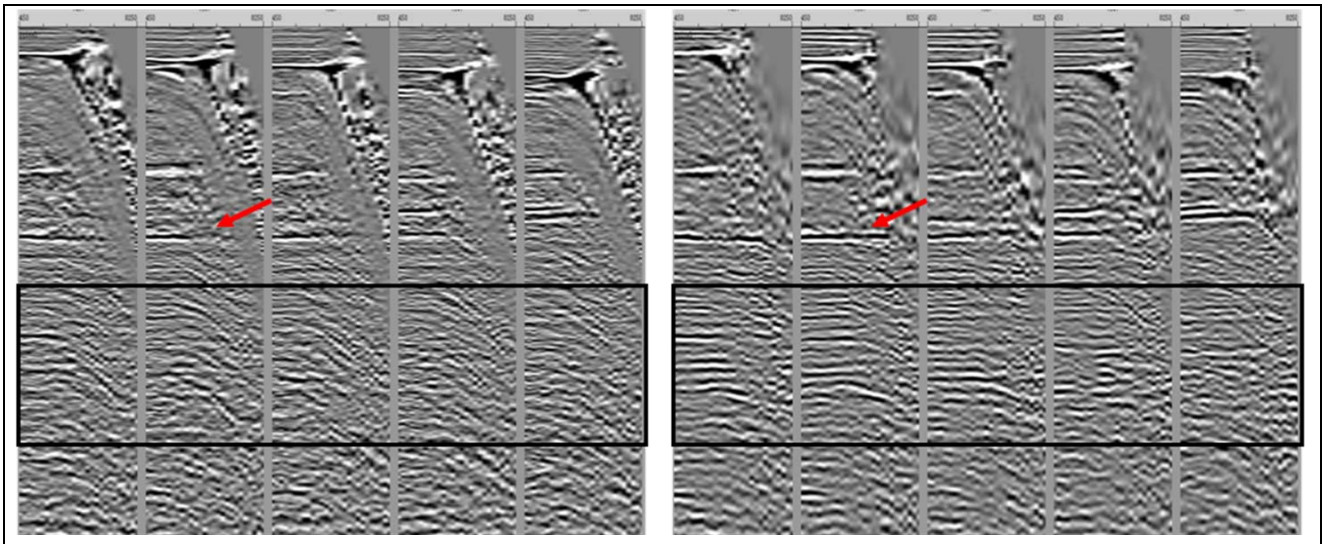

(a) Common image gathers from Kirchhoff (b) Common image gathers from CBM

Figure 2: Comparison of common image gathers of (a) Kirchhoff migration and (b) Controlled Beam migration at the middle subsalt area in figure 1. The offset ranges from 350m to 8km, with 150m increment.

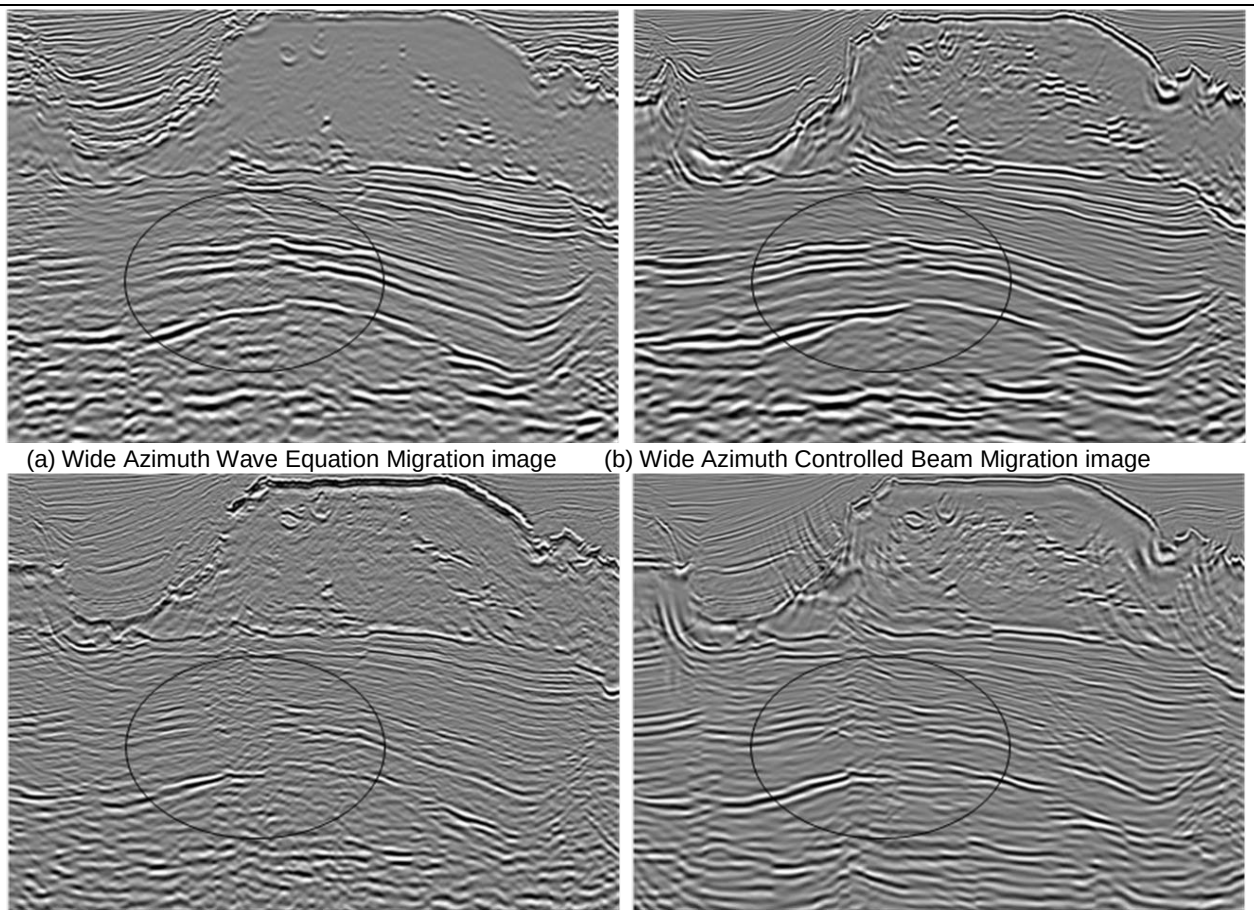

(a) Wide Azimuth Wave Equation Migration image (b) Wide Azimuth Controlled Beam Migration image

(c) Narrow Azimuth Wave Equation Migration image (d) Narrow Azimuth Controlled Beam Migration image

Figure 3: Comparison between WEM and CBM on both NAZ and WAZ data.

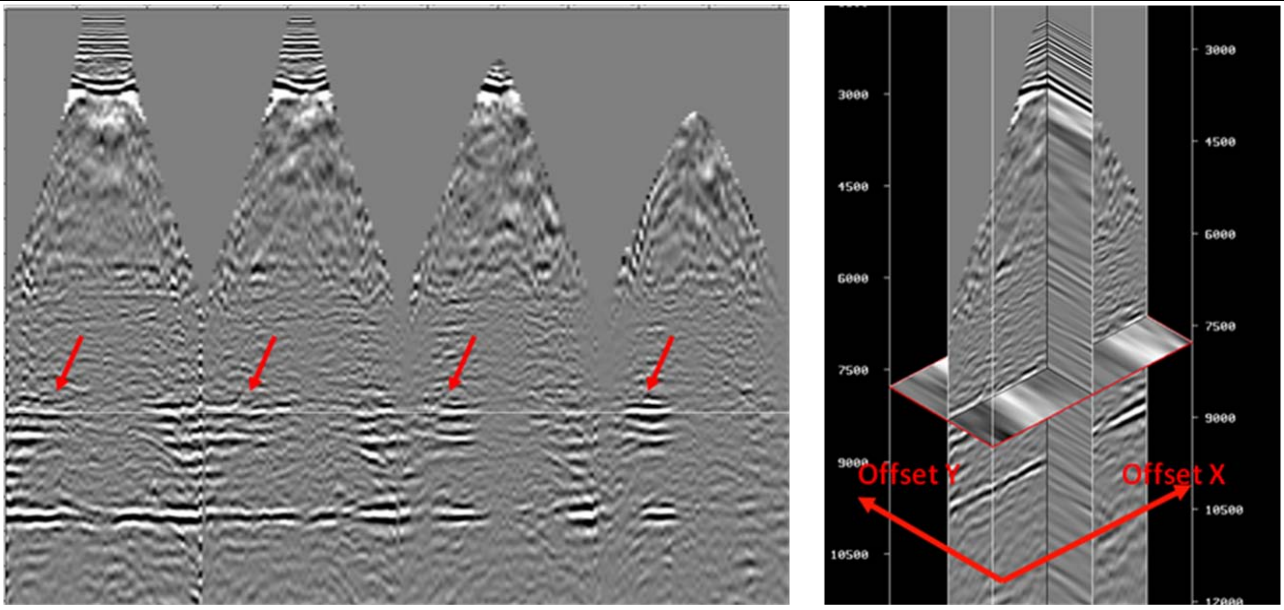

(a) 2D tiles panel view – from left to right, 1st tile to 4th tile (b) 3D vector offset volume view

Figure 4: One CBM migrated common image gather displayed in 2 different views. (a) 2D tiles panel view and (b) 3D vector offset volume view. The event marked by the arrows at 7.5km depth in (a) is shown as white spots in the depth slice at (b).